

## MODELLING OF LOCAL MELTING DURING FRICTION STIR WELDING OF Al-Zn-Mg ALLOYS

B. I. Bjørneklett\*, Ø. Frigaard\*, Ø. Grong\*, O. R. Myhr\*\* and O. T. Midling\*\*\*

\* The Norwegian University of Science and Technology N-7034, Trondheim, Norway

\*\* Hydro Raufoss Automotive Research Centre, N-2831, Raufoss, Norway

\*\*\* Hydro Aluminium, R&D Materials Technology, N-4265 Håvik, Norway

### ABSTRACT

The conditions for local melting at high angle grain boundaries during rapid heating of an Al-Zn-Mg alloy have been modelled. The initial size of the equilibrium  $\eta$ -phase has been established through transmission electron microscopy. Local melting occurs spontaneously if the particles are not fully dissolved when the eutectic temperature is reached. In the present paper the phenomenon is discussed in relation to friction stir welding, where local melting may be a limiting factor with respect to heat generation under the tool shoulder.

**Keywords:** *Aluminium, local melting, modelling, friction stir welding*

### 1. INTRODUCTION

Industrial processes such as extrusion, hot forming and welding involve rapid heating of the material. During these operations, local melting occurs if an alloy is heated above the eutectic temperature at a rate that does not allow the particles to fully dissolve into the matrix. Local melting will often have a detrimental effect on the high-temperature mechanical properties of the material, since the liquid is unable to support stress. As a result, hot deformation above the eutectic temperature becomes difficult.

The phenomenon of local melting has been studied in numerous alloy systems e.g. in connection with welding of maraging steel [1], 70Cu-30Ni alloy [2,3] and age hardenable aluminium alloys [4,5,6,7]. Some of the research dealing with local melting has also been directed towards extrudability of aluminium alloys within the 6xxx and 7xxx series [8,9]. Investigations in this field have lead to optimisation of the extrusion process through tight temperature control during billet preheating and extrusion.

The main objective of the present investigation is to examine a commercial Al-Zn-Mg extrusion with respect to local melting during rapid heating in the region between the eutectic temperature and the solidus temperature of the material. The emphasis is on friction stir welding (FSW), where the indications are that the heat generation under the tool shoulder may be limited by the presence of low melting eutectics at the steel/matrix interface [10,11]. The characteristic non-isothermal nature of the FSW process has, in turn, brought about the development of a numerical model for the dissolution of the primary constituent situated at high angle grain boundaries during rapid heating. The model may provide valuable insight into factors controlling the HAZ microstructure evolution. Moreover, since the size and distribution of the primary constituent phases in the base material are governed by the thermal history of the alloy, the results of this investigation can also serve as a basis for optimising welding performance through a change in the heat treatment procedure.

## 2. MATERIAL AND EXPERIMENTAL PROCEDURE

The nominal composition of the AA 7030 alloy is given in Table 1. In general, Al-Zn-Mg alloys can be welded in different temper conditions, i.e. T4, T6 or T7. In this investigation, the material used in the peak-aged (T6) condition. Thus, prior to weld thermal simulation the base material was subjected to a homogenisation treatment at 480°C for 20 minutes followed by quenching in water. A two step ageing treatment (100°C at 5 h and 150°C at 6 h) was then employed to obtain the desired T6 strength.

Table 1. Nominal alloy composition (in weight percent).

Alloy	Si	Fe	Cu	Mn	Mg	Zn	Ti	Al
AA 7030	0.05	0.12	0.30	0.01	1.18	5.26	0.03	balance

### 2.1 Weld Thermal Simulation

A Smith-Weld™ thermal simulator was used in order to evaluate the microstructural response of the material to rapid heating. The specimens (5 mm x 5 mm x 150 mm) were machined from the T6 tempered material. They were subsequently resistance-heated in the simulator at different rates up to a peak temperature of 550°C. After a short isothermal hold for 2.5 sec, the specimens were rapidly cooled down to room temperature at a rate of approximately 100°C/sec. The metallographic samples were taken from the centre of the specimens close to the location of the thermocouple.

### 2.2 TEM and Optical Microscopy

The TEM thin foils from the base material were prepared using a standard electropolishing technique. Moreover, the samples examined in the optical microscope were ground and polished down to a surface-finish of about 1 µm. A thin anodised layer was then deposited on the top of the specimen to reveal the microstructure in polarised light.

## 3. RESULTS AND DISCUSSION

The microstructure of the base material is shown in Figure 2. A closer examination in TEM reveals that the high angle grain boundaries are decorated by the equilibrium  $\eta$ -phase-(MgZn<sub>2</sub>), see Figure 3. These are approximately 15-20 nm wide and 40-60 nm long. However, the particles are not uniformly distributed throughout the material, i.e. some grain boundaries are more densely populated with particles than others. Outside and parallel to the grain boundary in Fig. 3 a precipitation free zone (PFZ) is visible, which is typical of age hardened 7xxx alloys. The small particles within the matrix are a mixture of the coherent  $\eta'$ -phase and GP-zones.

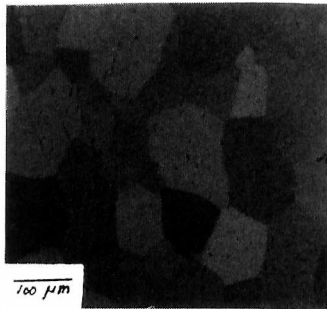


Figure 2. Microstructure of the base material.

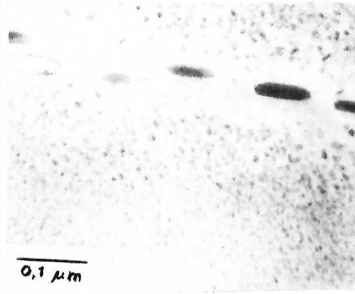


Figure 3. TEM image of a high angle grain boundary in the base material.

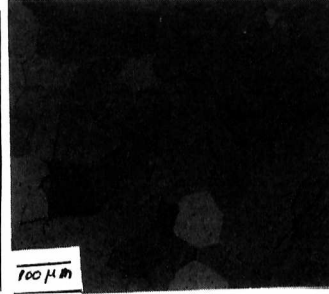


Figure 4. Microstructure after heating to 550°C at a constant rate of 330°C/s.

### 3.1 Weld Simulation Experiments

Clear evidence of local melting was found in several of the weld-simulated specimens. However, the degree of reaction depends upon the applied heating rate. Figure 4 shows the resulting microstructure after heating at a rate of 330 C°/s. During cooling, the liquid will solidify and form a black film along many of the grain boundaries. When the heating rate is reduced to 100°C/s, only some of the grain boundaries are decorated. From this it is obvious that the melting reaction occurs gradually over a range of heating rates, because local effects such as particle size and number density will finally determine the degree of melting achieved.

### 3.2 Modelling of Eutectic Melting

In the present investigation a numerical diffusion model, based on the finite difference approach, has been adopted in order to simulate the dissolution behaviour of the grain boundary precipitates under non-isothermal conditions [12]. A summary of input parameters used in modelling exercises is given in Table 2.

Table 2. Summary of input data used in the diffusion model.

Solvus boundary <sup>†</sup>		Diffusion coefficient <sup>‡</sup>		Starting conditions			
$C^*$ (wt %)	$\Delta H^o$ (kJ mol <sup>-1</sup> )	$D_o$ (μm <sup>2</sup> s <sup>-1</sup> )	$Q$ (kJ mol <sup>-1</sup> )	Particle (μm)	PFZ (μm)	$C_p$ (wt %)	$C_o$ (wt %)
$5.2 \times 10^2$	22.44	$1.05 \times 10^8$	127.9	0.016	0.05	100	6

$$^{\dagger} C_i = C^* \exp\left(-\frac{\Delta H^o}{RT}\right) \quad ^{\ddagger} D = D_o \exp\left(-\frac{Q}{RT}\right)$$

The model assumes a planar particle geometry and that the dissolution rate is controlled by the slowest diffusing atom in the matrix, without any interaction with other constituent atoms. Since the reported diffusion data for Zn and Mg in Al fall within the same scatter band [9], the choice of Zn as the rate controlling element is not critical in the sense that it alters the outcome of the analysis. Moreover, the solvus-boundary enthalpy refers to the quasi-binary section of Al-Zn-Mg phase diagram. The other input data, such as initial particle size and width of the PFZ, are obtained from the TEM investigation. The predicted change in the concentration profile outside the particles, as a function of time, is shown in Figure 5. It follows that the PFZ itself does not have a large influence on the dissolution process, because solute will rapidly be supplied from the adjacent matrix during the initial stage of heating.

### 3.3 Application to FSW

In FSW of aluminium alloys the friction coefficient  $\mu$  will change continuously during heating of the base material [10,11], from  $\mu > 1$  for dry sliding towards zero when a liquid film is present at the tool/matrix interface. As shown in Fig. 7, the temperature at which this occurs will depend on the actual heating rate ahead of the tool shoulder. If the conditions for local melting are met, the maximum temperature  $T_{max}$  is close to 475°C. Otherwise,  $T_{max}$  will approach the solidus temperature of the alloy.

As shown by the simulation results in Fig. 8, using the 3-D numerical heat flow model of Frigaard *et al.* [11], an increase in  $T_{max}$  from 475 to, say, 607°C will have a dramatic effect on the temperature distribution during FSW and the resulting width of the HAZ. This, in turn, may affect the welding performance and eventually the mechanical integrity of the joint [10,11].

It follows that high strength Al-Zn-Mg alloys (such as AA 7075) should be particularly prone to the form of liquation, because they usually contain a high proportion of grain boundary precipitates in the age-hardened condition. In practice, the problem can be overcome by increasing the applied heat input during welding so that the particles are allowed to dissolve before the eutectic temperature is reached.

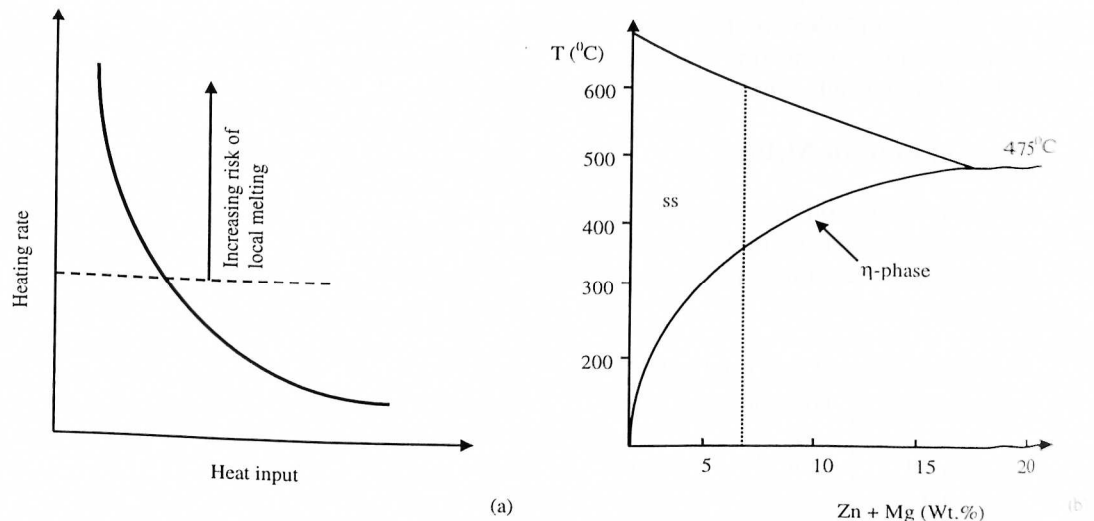


Figure 7. Conditions for local melting during FSW of Al-Zn-Mg alloys (schematic); (a) Effect of heat input on the heating rate ahead of the tool shoulder, (b) Quasi-binary section of the Al-(Zn+Mg) phase diagram.

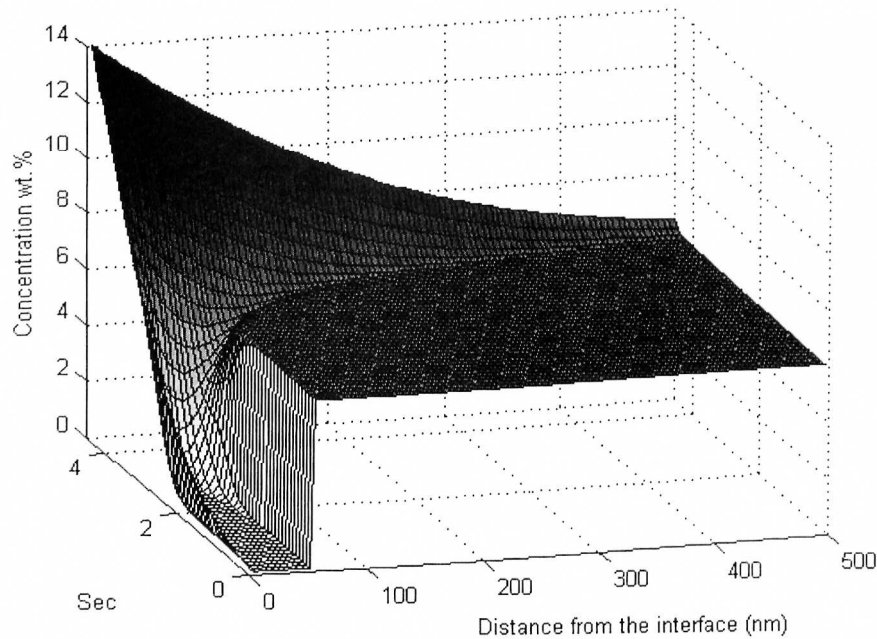


Figure 5. Predicted solute concentration profiles in the near vicinity of the particles during heating to 550°C at a constant rate of 100 °C/s.

By considering the total area under the concentration profile and correcting for the matrix concentration, the fraction dissolved can be calculated as shown in Figure 6.

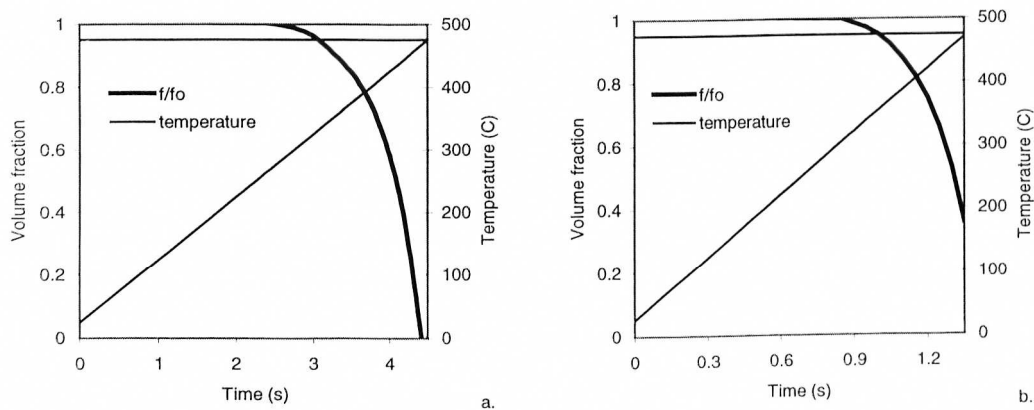


Figure 6. Predicted fraction dissolved  $f/f_0$  as a function of time during linear heating at two different rates; a) 100°C/s, and b) 330°C/s.

Referring to Fig. 6a, heating at a rate of 100°C/s implies that the dissolution process is completed before the eutectic temperature is reached at 475°C, indicating that no melting will take place for this particle size. However, if the heating rate is increased to 330°C/s (Fig. 6b), only about 70% of the particle has dissolved, which provides the necessary condition for local melting. The results from these simulations agree well with the experimental observations in Fig. 4.

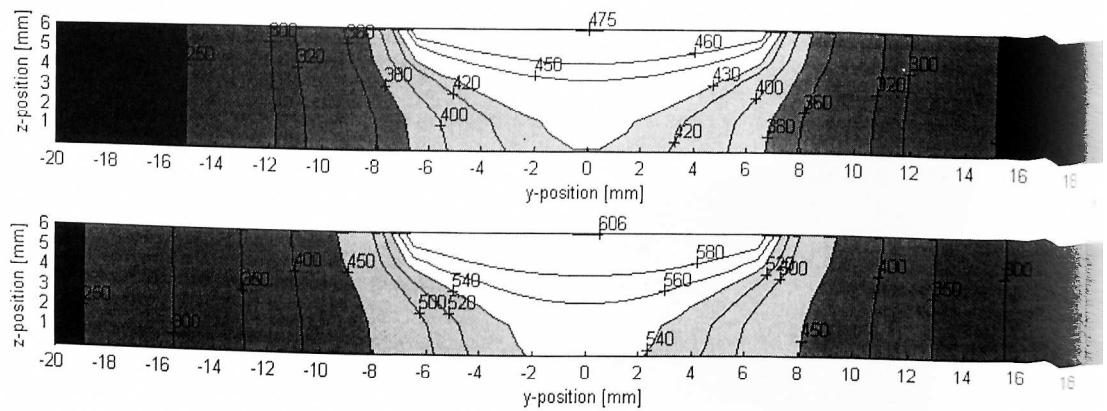


Figure 8. Computed peak temperature contours in the cross section of AA 7030 friction weldments at pseudo-steady state; (a)  $T_{max} = 475^{\circ}\text{C}$ , (b)  $T_{max} = 607^{\circ}\text{C}$ . Assumed operating conditions: Plate dimensions: 100 mm x 150 mm x 6 mm, welding speed: 8 mm/s, shoulder radius 8 mm, net power of heat source: 800 W.

#### 4. ACKNOWLEDGEMENTS

The authors acknowledge the financial support from the Norwegian Research Council and Hydro.

#### 5. REFERENCES

- [1] J. J. Pepe, Ph.D. Thesis, Rensselaer Polytechnic, (1966), New York, USA
- [2] W. F. Savage, E. F. Nippes and T. W. Miller, J. Weld. Res. Sup. 46, (1976), 181
- [3] V. L. Acoff, R. G. Thompson, Conf. proc. 4th Trends in welding research, (1995), 241, USA.
- [4] S. Kou, *Welding Metallurgy*, J. Wiley & Sons, (1987), USA,
- [5] V. Malin, J. Weld. Res. Sup. 74, (1995), 305
- [6] A. Katoh and H. W. Kerr, J. Weld. Res. Sup. 65, (1987), 360
- [7] N. F. Gittos and M. H. Scott, J. Weld. Res. Sup. 49, (1981), 95
- [8] O. Reiso, J. Strid and N. Ryum, Met. Trans. 21A, (1990), 1689
- [9] P. E. Drønen and N. Ryum, Met. Trans. 25A, (1994), 521
- [10] Ø. Frigaard, Ø. Grong and O. T. Midling, Proc. 7<sup>th</sup> INALCO (1998), UK
- [11] Ø. Frigaard, B. Bjørneklett, Ø. Grong and O. T. Midling, Proc 6<sup>th</sup> ICCA, (1998), Japan
- [12] O. R. Myhr, Ph.D. Thesis, Norwegian Institute of technology, (1990), Trondheim, Norway